Advanced Numerical Study of the Response of Orthotropic Steel Deck Bridge with Two Membrane Layers System

J. Li, X.Liu, A.Scarpas, G.Tzimiris
(Delft University of Technology, Stevinweg 1, 2628 CN Delft, the Netherlands, Jinlong.li@tudelft.nl)

ABSTRACT

In the Netherlands an asphaltic surfacing structure for orthotropic steel bridge decks mostly consists of two structural layers. The upper layer consists of Porous Asphalt (PA) because of reasons related to noise hindrance. For the lower layer a choice between Mastic Asphalt (MA) or Guss Asphalt (GA), can be made. In this paper, a typical Dutch steel bridge deck surfacing system is simulated by means of the three-dimensional finite element system CAPA 3D. Special attention is given to the structural distress phenomena and the parameters that influenced them. The FE model shows the distribution of strains and stresses inside the surfacing materials depends highly on the wheel load level, wheel load frequency, wheel position, membrane bonding strength as well as the thicknesses and the characteristics of the surfacing layers.

Keywords: orthotropic steel bridge; membrane; surfacing; finite element.

1 INTRODUCTION

Light weight orthotropic steel bridge decks have been widely utilized for bridges in seismic zones, movable bridges and long span bridges. Nowadays more than 1000 orthotropic steel bridges have been built in Europe, out of which 86 are in the Netherlands [1]. In Asia, there are several orthotropic steel bridges that are built or being built, especially in China and Japan [2].

In the Netherlands an asphaltic surfacing structure for orthotropic steel bridge decks mostly consists of two structural layers. The upper layer consists of PA because of reasons related to noise hindrance. For the lower layer a choice between MA, or GA, can be made. Mostly, different membrane layers are involved, functioned as bonding layer, isolation layer as well as adhesion layer [3]. Earlier works done by [1-6] have shown that the shear stiffness of membrane layers bonded to the surrounding materials has significant influences on the structural response of orthotropic steel bridge decks. The most important requirement for the application of membrane materials on orthotropic steel bridge decks is that the membrane adhesive layer shall be able to provide sufficient bond to the surrounding materials.

In the last three decades, several problems were reported in relation to asphaltic surfacing materials on orthotropic steel deck bridges such as rutting, cracking, loss of bond between the surfacing material and the steel plate. The severity of the problems is enhanced by the considerable increase in traffic in terms of number of trucks, heavier wheel loads, wide-base tires etc. Current design methods have a very limited success in estimating correctly the life span of the surfacing material.

For the aforementioned reasons the Dutch Transport Research Centre (DVS) of the Ministry of Transport, Public Works and Water Management (RWS) commissioned the Delft University of Technology together with TNO to execute a research plan into membrane performance on steel bridge decks. The research aims on improving the performance of asphaltic surfacing structures so that their service life increases to an average of eight years. Focus is on membrane performance and the effects hereof on the structure as a whole.

In this paper, finite element (FE) simulations of Merwede bridge with two membrane layers system are presented. The finite element system CAPA-3D [7] developed at the Section of Structural Mechanics of TU Delft has been utilized as the numerical platform for this study. Due to the multilayer of the surfacing materials and geometrical complexity of the steel bridge, the FE

model shows the development of strains and stresses inside the membrane layers depends highly on the wheel loading frequency, wheel position, membrane bonding strength as well as thicknesses and characteristics of the surfacing layers. Results of both static and dynamic FE simulations under different loading conditions are presented and discussed. Special attention is given to identify the critical wheel load location, maximum tensile stress distribution and the variation of strain rate inside the membrane layers.

2 BRIDGE DESCRIPTION AND FINITE ELEMENT MODELS

2.1 The bridge of concern

The Merwede bridge, locates in the A27 near Gorinchem, was opened on March 15 1961 by Queen Juliana. Over the past fifty years, this bridge has been playing very important role in connecting traffic between Randstad and North Brabant. Over 100,000 vehicles pass through the bridge every day as well as many cyclists. The Merwede bridge steel deck was constructed with open longitudinal stiffeners placed each 300mm. Crossbeams were placed every 2m and with 10mm thick steel deck plate [Figure 1].

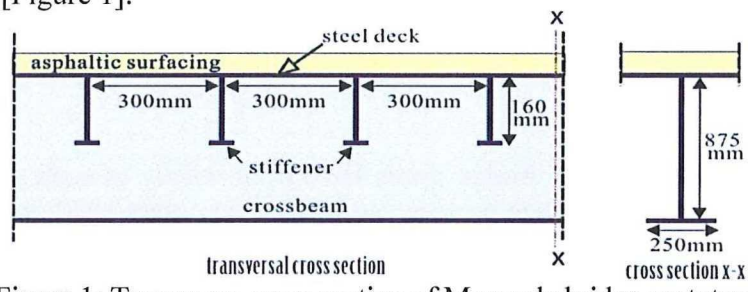

Figure 1: Transverse cross-section of Merwede bridge prototype

2.2 Finite element models

Two structural FE models of the Merwede bridge were utilized. One model makes use of symmetry in a vertical plane perpendicular to the direction of the bridge span, see Figure 2(a). Due to the use of symmetry, the required computation time to determine the stresses and strains in the bridge panel is reduced. An apparent disadvantage is that loads can only be applied at the plane of symmetry. The second model involves a complete mesh of the bridge with two span. This model can give us full freedom to change the traffic load locations on the bridge, see Figure 2(b).

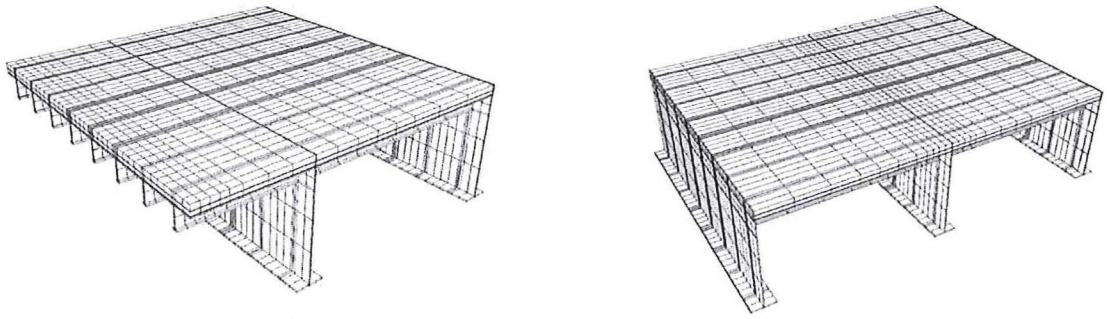

(a) FE model of one and half span bridge (b) FE model of two span bridge

Figure 2: FE meshes for modeling the Merwede bridge

A dual wheel load is applied on the surface asphalt concrete layers. Each individual tyre of the wheel load has a contact area that is 220 mm wide and 320 mm long (Eurocode 1-3). There is a 60 mm

spacing between two tyres fitted on one wheel. The contact pressure was set to be 0.707MPa, resulting in a 200 kN axle load. The wheel load configuration and the transversal location on the bridge are shown in

Figure 3 and
Figure 4.

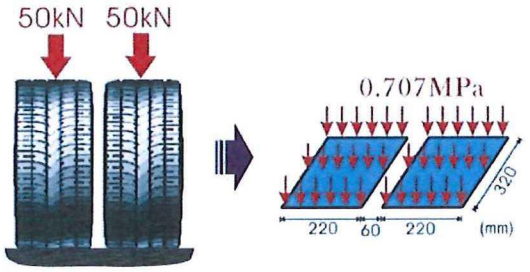

Figure 3: Dual wheel loading

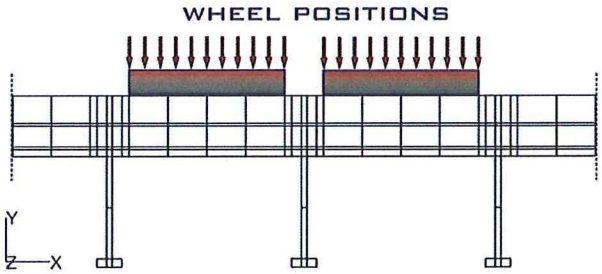

Figure 4: dual wheel load positions on FE mesh

The bridge FE mesh consists of two asphalt concrete layers, two membrane layers and four interface layers, see Figure 5. The upper layer represents a layer of porous asphalt concrete with a thickness of 40mm. The lower asphalt concrete layer consist of Guss asphalt with thickness of 30mm. Two membrane layers have same thickness of 3mm. In the simulation, interface elements have been introduced to simulate the discontinuity between the different surfacing layers. The bond stiffness of the interfaces is assumed to be 0.1 N/mm/mm^2. The basic material liner elasticity parameters are shown in Table 1.

Table 1: Material elasticity properties

Material	E modulus [MPa]	Poisson's ratio
steel	2100000	0.2
Guss asphalt	7000	0.35
porous asphalt	5500	0.35
top membrane	100~300	0.3
bottom membrane	100~300	0.3

In order to investigate the influence of the wheel load location on the bridge structure response, three cases of load location have been investigated:

Case 1: a dual wheel load is applied on top of the porous asphalt concrete layer at midway between two successive crossbeams, see Figure 6.

Case 2: a dual wheel load is applied on top of the porous asphalt concrete layer positioned directly on a crossbeam, see Figure 7.

Case 3: a dual wheel load is applied on top of the porous asphalt concrete layer positioned right next to a crossbeam, see Figure 8.

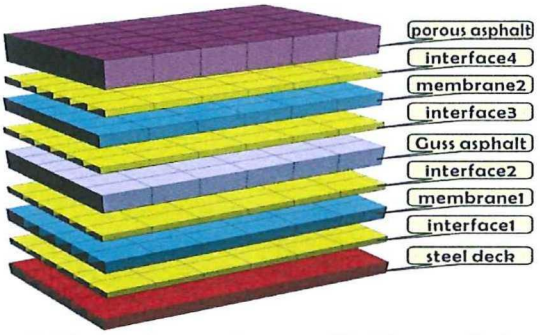

Figure 5: Finite element layers of bridge surfacing system

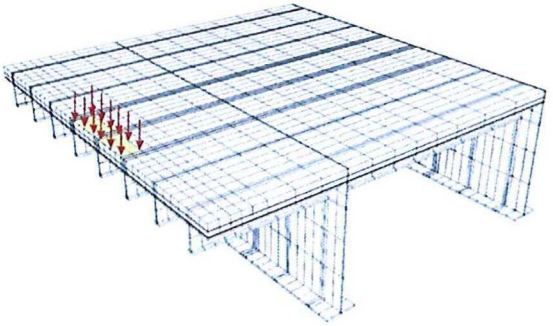

Figure 6: The mesh for load placed midway between crossbeams (case 1)

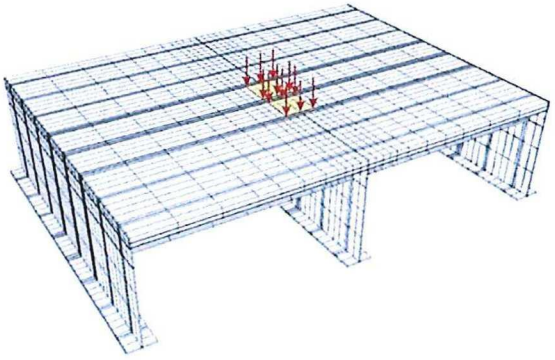

Figure 7: the mesh for load placed on one crossbeam (case 2)

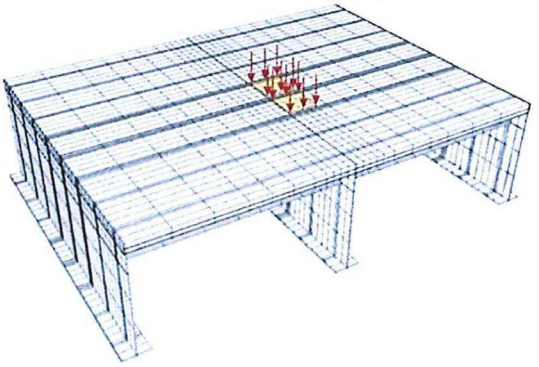

Figure 8: the mesh for load placed next to a crossbeam (case 3)

For each load position, two types of load are simulated. One is the static linear increasing load, see Figure 9a. Another one is the dynamic harmonic beat load, see Figure 9b.

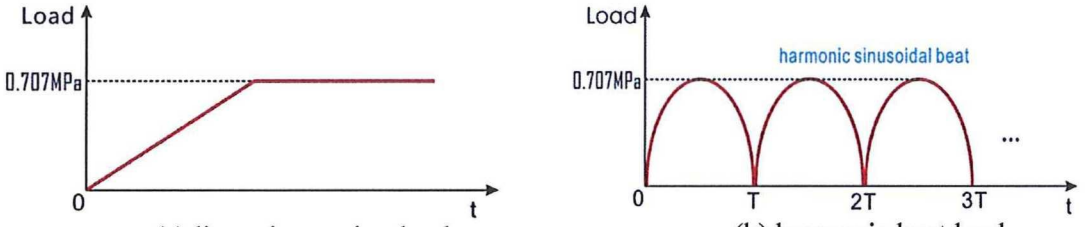

(a) linear increasing load (b) harmonic beat load

Figure 9: Two types of wheel load

In the following, the response of the bridge structures subjected to wheel load at above three different locations is investigated and some general conclusions are then drawn.

3 THE RESPONSE OF THE BRIDGE AT VARIOUS LOAD CONDITIONS

3.1 load positioned midway between two successive crossbeams (case 1)

The distributions of stress yy (perpendicular to bridge surfacing) at the bottom membrane and the top membrane layer are shown in Figure 10 and Figure 11 respectively.

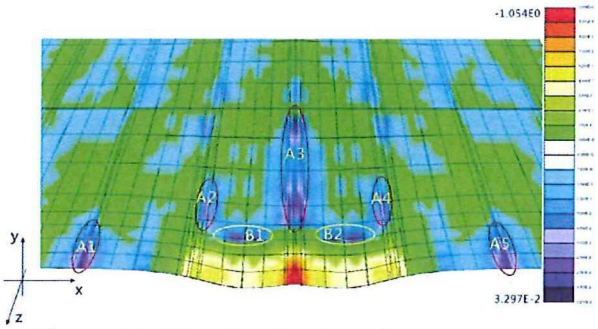

Figure 10: The distribution of stress yy at the bottom membrane layer

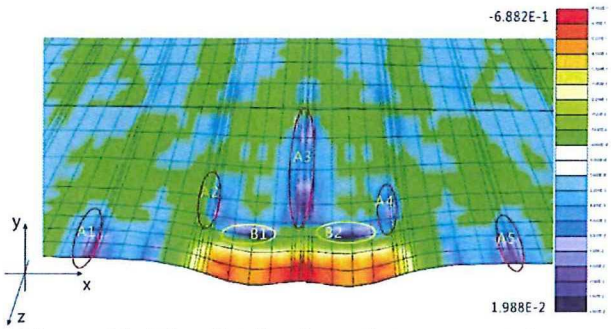

Figure 11: The distribution of stress yy at the top membrane layer

From Figure 10 and Figure 11 the following observations are made:

- The bottom membrane sustains both higher tensile and compressive stresses than the top membrane;
- The distribution of the stress along x-axis is more or less symmetrical around the middle of the dual wheel load;
- High tensile stresses occur at the membranes which are laid on the top of open stiffeners (A1,A2,A3,A4,A5);
- High tensile stresses are also found at the places midway between stiffeners where the wheel loads are applied (B1,B2). They occur beside the wheel loads rather than under them.

In order to find the most critical stress points, stresses in three orthogonal directions named $\sigma_{xx}, \sigma_{yy}, \sigma_{zz}$ in the bottom membrane layer are plotted in Figure 12.

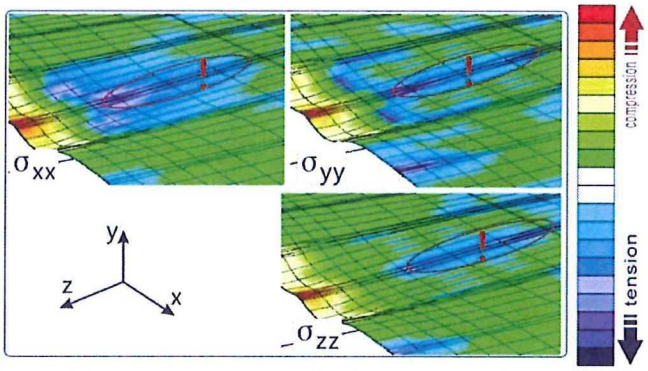

Figure 12: $\sigma_{xx}, \sigma_{yy}, \sigma_{zz}$ at the bottom membrane (case 1)

Figure 12 shows the location with exclamation mark where all the three stress components are in tension with the highest values. This is the critical place that membrane may have potential to loose bonding strength.

In order to study the influence of membrane stiffness on the maximum tensile stress development in the membrane layers, simulations with membrane stiffness equals to 100MPa, 200MPa, 300MPa are investigated under both static and dynamic loading conditions, see Figure 9. The distributions of stress yy of static and dynamic simulations at the critical position shown in Figure 12 are plotted in Figure 13 and Figure 14Figure 15 respectively.

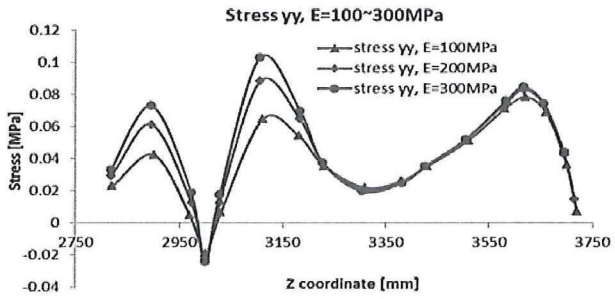

Figure 13: tensile stress yy at the bottom membrane (case1, static)

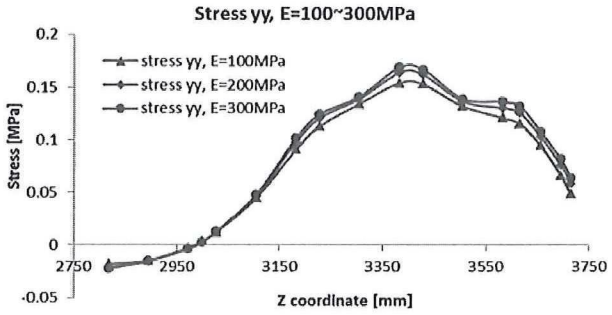

Figure 14: tensile stress yy at the bottom membrane (case1, dynamic)

It can observed that, for static simulation, the maximum tensile stress of 0.11MPa is obtained, while for dynamic simulation, the maximum tensile stress in the bottom membrane is around 0.17MPa. The static simulation is useful to provide a global picture of the strain/stress fields in the structure. However the dynamic simulation is more close to the real bridge situation.

Figure 15 illustrates the distribution of stress yy and strain yy in the bottom membrane layer directly under the wheel load over the width of the bridge deck section.

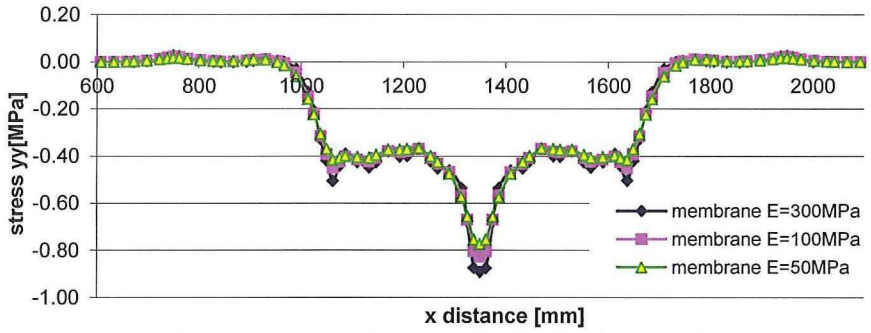

Figure 15: Stress yy at the bottom membrane under dual wheel load along transversal section

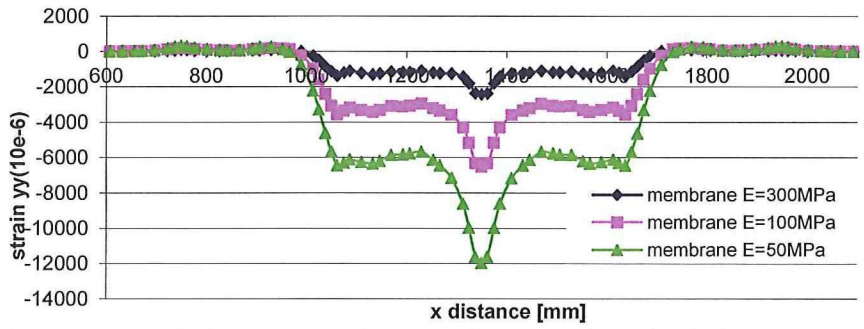

Figure 16: strain yy at the bottom membrane under dual wheel load along transversal section

By comparing Figure 15 together with Figure 16, the following observations and conclusions are made:

- The stiffness of membrane doesn't influence very much on the stress yy distribution inside the bottom membrane. The peak compression stress (0.85 MPa) occurs in the middle of the dual wheel where a stiffener is placed.
- The peak compression stress is higher than the dual wheel load 0.707MPa, that's because of stress concentration due to high stiffness of stiffeners.
- By comparison stress distributions between upper and lower membranes, it is found that the peak stress in the lower membrane is higher than that of upper layer. This phenomenon can

be explained by stress concentration because the lower membrane layer is closer to the stiffener so that severer concentration is achieved.

- By adjusting the membrane E from 50MPa to 300MPa, strain distributions inside the bottom membrane differ a lot.

3.2 Load positioned on a crossbeam (case 2)

When wheel load is applied on the crossbeam location, the distribution of stress yy at the bottom membrane is shown in Figure 17. The following observations are made:

- High tension stresses are found on top of the crossbeam, right beside the wheel load position (A1, A2);
- High tension stress occurred also at midway between stiffeners next to the loading position (B1, B2, B3, B4).

Similar as case 1, Figure 18 shows a location with exclamation mark where all the three stress components are in tension with the highest values. This is the critical place that membrane will have potential to have debonding failure.

In order to study the influence of membrane stiffness on the maximum tensile stress development inside the bottom membrane layers, Simulations with membrane stiffness equals to 100MPa, 200MPa and 300MPa have been done under both static and dynamic loading conditions. The distributions of stress yy at the critical point are plotted in Figure 19 and Figure 20 respectively.

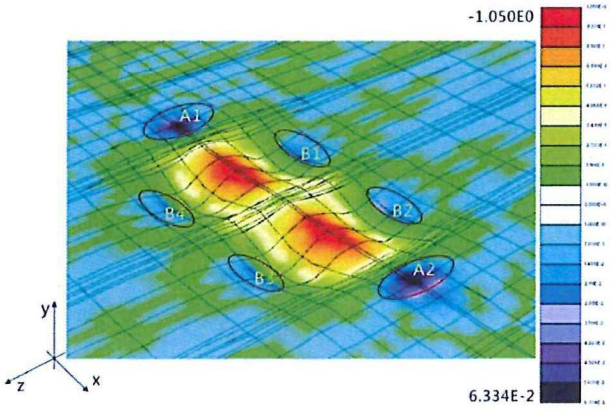

Figure 17: the distribution of stress yy at the bottom membrane layer

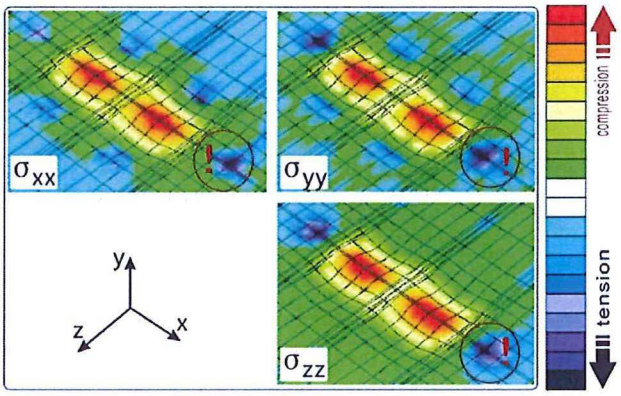

Figure 18: $\sigma_{xx}, \sigma_{yy}, \sigma_{zz}$ at the bottom membrane layer

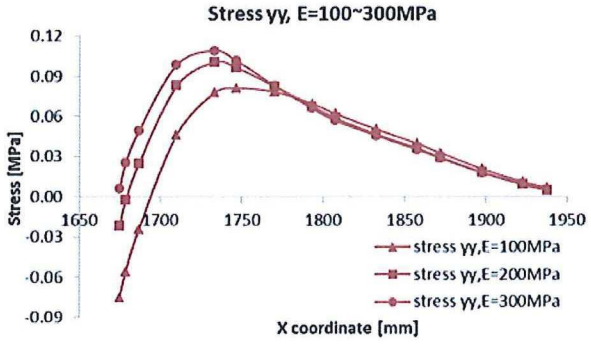

Figure 19:tensile stress yy at the bottom membrane (case2, static)

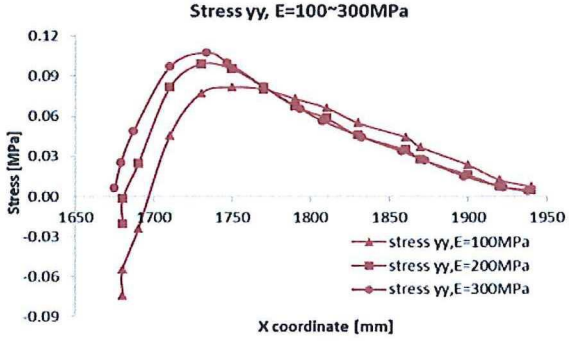

Figure 20: tensile stress yy at the bottom membrane (case2, dynamic)

The following observations are made.

- The distributions of the stress $\sigma_{xx}, \sigma_{yy}, \sigma_{zz}$ of static and dynamic load simulations follow more or less the same pattern when wheel load is symmetrically applied on the crossbeam. Because of the higher stiffness of crossbeam, the influence of the dynamic load has less influence than the case 1.
- High tensile stress is found around 0.11MPa for both static and dynamic loading conditions.
- Stiffer membrane undergoes higher tensile stress, but the differences between stiffer and softer cases are not obvious.

3.3 Load positioned next to a crossbeam (case 3)

Figure 21 shows the contour plot of stress yy at the bottom membrane layer of case 3. The following observations can be made.

- The distribution of the stress follows more or less the same pattern as in case 2. The critical higher tensile stress point A0 is found at place where the bridge deck is supported by stiffeners or cross beams, around the wheel load, see Figure 21 .
- The higher tensile stress concentration at point A0 is mainly due to the higher stiffness difference between asphalt layer above the membrane and steel stiffener bellow.

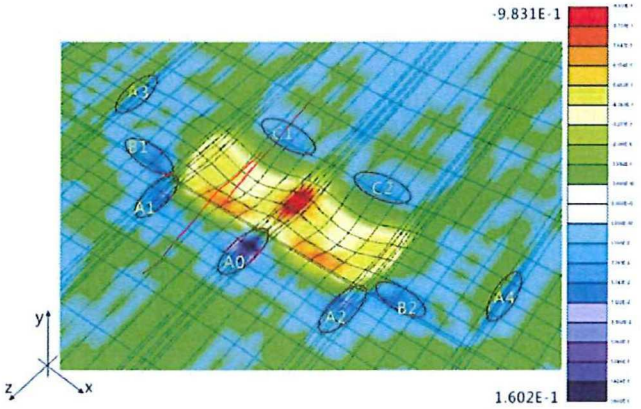

Figure 21: distribution of stress yy at the bottom membrane layer (case 3)

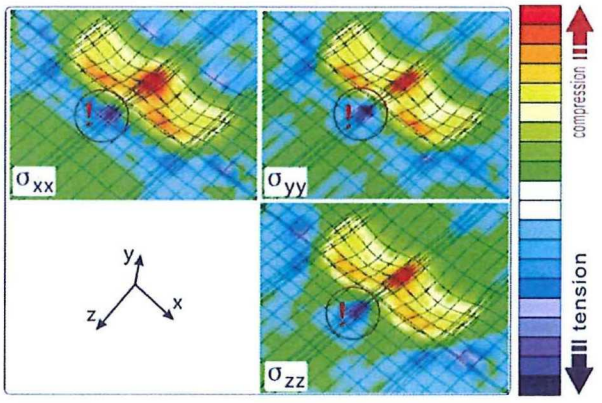

Figure 22: $\sigma_{xx}, \sigma_{yy}, \sigma_{zz}$ at the bottom membrane (case 3)

Figure 22 illustrates the location with exclamation mark where all the three stress components are in tension with the higher values.

Figure 23 and Figure 24 show the distributions of stress yy at the critical stress point in Figure 22 under both static and dynamic loading conditions.

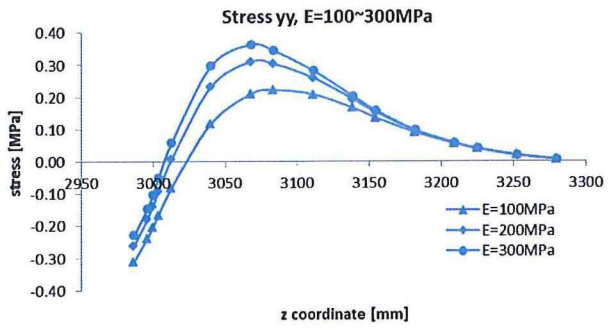

Figure 23: tensile stress yy at the bottom membrane (case3, static)

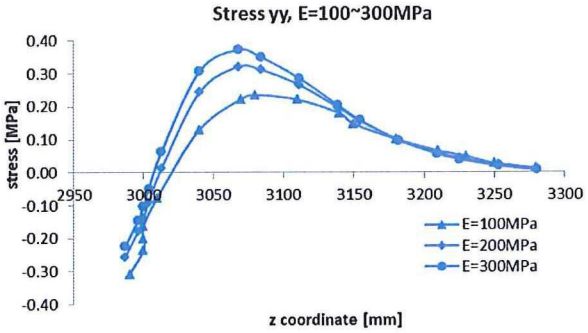

Figure 24: tensile stress yy at the bottom membrane (case3, dynamic)

The following observations are made:

- The distributions of the stress σ_{yy} of static and dynamic load simulations follow more or less the same pattern The response of dynamic case is only 5% higher than that of static case.
- Stiffer membrane subjects to the higher tensile stress.

4 STRAIN RATE CALCULATION AND MOVING LOAD SIMULATION

The response of asphalt concrete surfacings and membrane layers depend highly on the strain rate and temperature distributions in the bridge. In order to characterize the surfacing material accurately, the magnitude of the reasonable strain rate in the bridge needs to be identified. In this study, the same bridge model as utilized in the previous section is chosen for the finite element simulation.

The FE mesh with symmetry in a vertical plane perpendicular to the direction of the bridge span is illustrated in Figure 25. A dual wheel moving load with 80km/h is applied on the top layer of the asphalt concrete. The the moving load location and boundary conditions are shown in Figure 26.

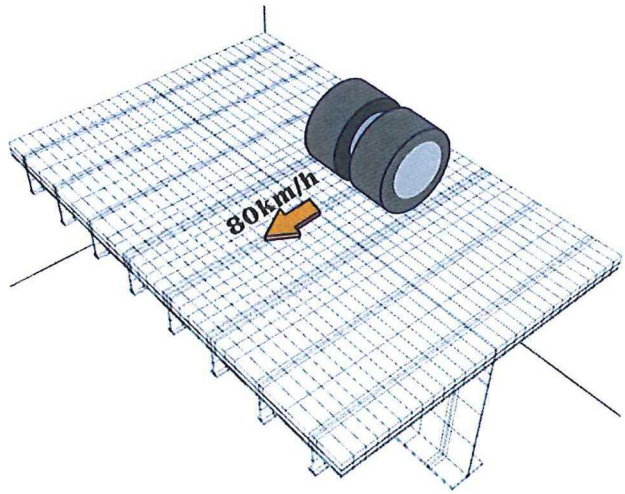

Figure 25: Mesh for simulation of moving load

In this study, the in time variations of tensile strain rate inside the membrane layers are identified. According to the numerical observations from the previous simulations with three different steady wheel load cases, the bottom membrane layer always undergo a higher strain/stress concentration. Therefore, to find maximum strain rate inside the membrane layers, attention has to be paid on the bottom membrane layer.

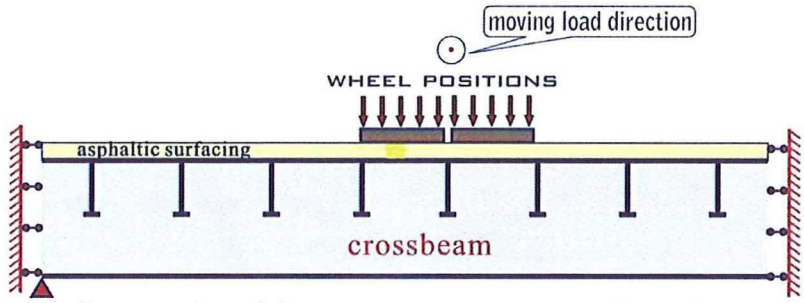

Figure 26: Cross section of the moving load location and boundary conditions

From contour plot of Figure 21, it is found that the highest tensile stress occurs at location A0 of the bottom membrane layer where the stiffener is welded with the crossbeam. The in time strain development at this location is plotted in Figure 27.

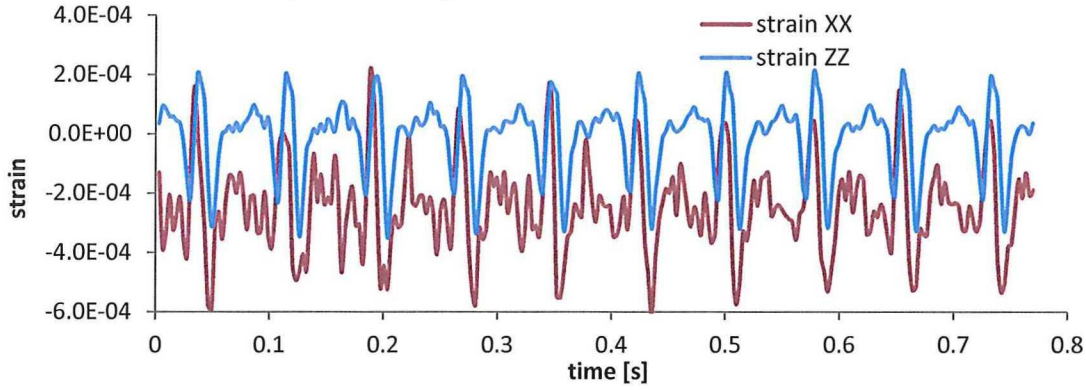

Figure 27: Horizontal strains in bottom membrane

It can be observed that periodic strain variation occurs at this critical point. By differentiation of the strains in Figure 27 with respect to time, the corresponding in time strain rate variations are obtained, see Figure 28.

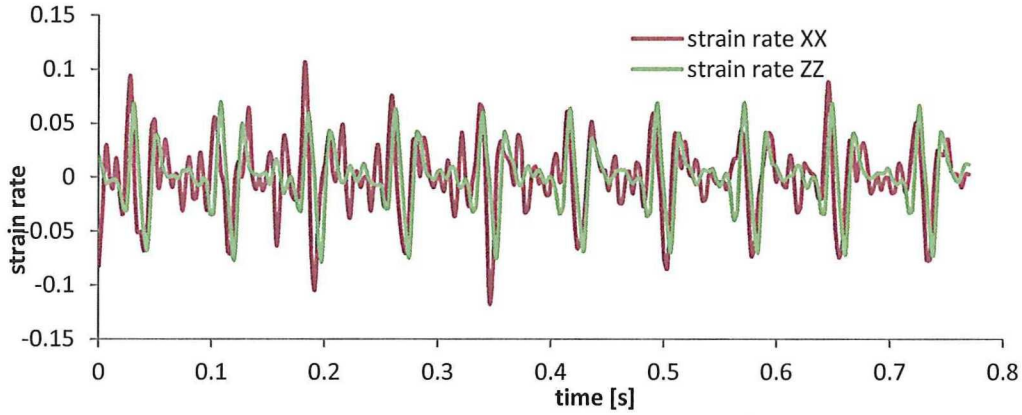

Figure 28: Development of strain rates inside membrane plane

From Figure 28 conclusion that the maximum membrane strain rate is about 0.1 can be drawn. This result provides us important information for experimental quantification of membrane products.

The details of using this strain rate to quantify membrane product can be found in the companion paper [9] in this conference.

5 CONCLUSIONS AND RECOMMENDATIONS

Based on the results presented in the paper, the following conclusions and recommendations can be made.

1. The FE models are capable of simulating the realistic behavior of orthotropic steel bridge. The properties of surfacing materials and the complexity of the bridge structure significantly influence the distribution of strains and stresses in the bridge.
2. Maximum tensile stress in membrane layer is found around 0.4MPa, which coincide with the minimum requirement for adhesive bonding strength of membrane material proposed by standard NF P98-282 and TP-BEL-B.
3. Maximum membrane strain rate is found around 0.1, which is an important information that can be utilized for characterization of membrane products.

ACKNOWLEDGMENT

This research project is funded by the Dutch Transport Research Centre (DVS) of the Ministry of Transport, Public Works and Water Management (RWS). Their financial support is highly appreciated.

REFERENCE

[1] Liu, X., Medani, T.O., Scarpas, A., Huurman, M. and Molenaar, A.A.A. "Experimental and numerical characterization of a membrane material for orthotropic steel deck bridges: Part 2 - Development and implementation of a nonlinear constitutive model," *Finite Elements in Analysis and Design,* vol. 44, pp. 580-594, June 2008.

[2] Medani, T. O. "Design principles of surfacings on orthotropic steel bridge decks," PhD, Delft University of Technology, Delft, 2006.

[3] Medani, T. O., Liu, X., Huurman, M., Scarpas, A. and Molenaar, A. A. A. "Experimental and numerical characterization of a membrane material for orthotropic steel deck bridges: Part 1 - Experimental work and data interpretation," *Finite Elements in Analysis and Design,* vol. 44, pp. 552-563, Jun 2008.

[4] Medani, T. O., Scarpas, A., Kolstein, M. H. and Molenaar, A. A. A. "Design aspects for wearing courses on orthotropic steel bridge decks," presented at the ISAP, Copenhagen, Denmark, 2002.

[5] Huurman, M., Medani, T. O., Scarpas, A. and Kasbergen, C. "3D-FEM for estimation of the behaviour of asphalt surfacings on orthotropic steel deck bridges," presented at the International Conference on Computational and Experimental Engineering and Sciences, Corfu, Greece, 2003.

[6] Huurman, M., Medani, T. O., Molenaar, A. A. A., Kasbergen, C. and Scarpas, A."3D-FEM for estimation of the behaviour of asphalt surfacings on orthotropic steel deck bridges," presented at the 83rd Annual TRB Meeting, Washington, DC, USA, 2004.

[7] Scarpas, A. & Liu, X. "CAPA-3D finite elements system user's manual, parts I, II and III," Department of Structural Mechanics, Faculty of Civil Engineering, Delft University of Technology, Delft, The Netherlands, 2008.

[8] Liu, X., Scarpas, A., Li, J. & Tzimirs, G. "Application of MAT device to characterize the adhesive bonding strength of membrane in orthotropic steel deck bridges," presented at ISAP international symposium, Nanjing, 2012